bond moment of 0.5 D will nicely raise μ_a and lower μ_c to the observed values only if the negative end is directed to the phosphorus with the fluorine substituents. This value suggests an inductive effect from the fluorines, and the direction of the bond dipole is consistent with the greater Lewis basicity toward borane of the phosphorus with the attached fluorines. It is interesting to note that the same value for the PP bond moment fits both μ_a and μ_c for H_2PPF_2, implying that the bond dipole moments in PF_3, PH_3, and H_2PPF_2 are internally consistent.

This investigation shows that the stable conformation is trans with no evidence for appreciable amounts of a gauche conformer. This is particularly interesting for two reasons. First, there appears to be no tendency for the lone pair on the PH_2 group to form a d_π–p_π bond to the PF_2 end since this would make the PH_2 group planar. This effect can be invoked to rationalize the planar arrangement around the nitrogen in H_2NPF_2[12] and $(CH_3)_2NPF_2$.[11] An analogy to this result has been observed with $N(SiH_3)_3$ which is planar[24] while $P(SiH_3)_3$ is pyramidal.[25]

Second, the stability of the trans form is interesting in view of the electrical asymmetry in H_2PPF_2; apparently an internal attraction between the hydrogens and fluorines is not influential enough to stabilize the gauche isomer. There is, however, some suggestion of an interaction involving the hydrogens since the PPH angle is a "small" 90°. Since H_2PPF_2 readily decomposes to HPF_2, it seems preferable to call the interaction an attraction presumably toward the lone pair on the adjacent phosphorus.

The data now available indicate that all gaseous diphosphines have the trans conformation except H_4P_2. A trans conformation seems readily justified invoking steric repulsion and/or lone pair interactions. These two effects should be the smallest in H_4P_2 so a gauche conformation would be more likely; nevertheless some stabilizing interaction must still operate to give the gauche conformation. The results of this investigation certainly suggest that further studies of the molecular and electronic structure of H_4P_2 and its potential function for rotation about the PP bond are warranted.

Acknowledgment.—This research was supported by a grant (GP 11388) from the National Science Foundation, Washington, D. C. We are also grateful to Professor R. H. Schwendeman for helpful discussions concerning the Stark effect. The sponsorship of H. W. S. by the Civilian Institutions Program, Air Force Institute of Technology, is gratefully acknowledged.

---

(24) B. Beagley and A. R. Conrad, *Trans. Faraday Soc.*, **66**, 2740 (1970).

(25) B. Beagley, A. G. Robiette, and G. M. Sheldrick, *J. Chem. Soc.*, 601 (1967).

CONTRIBUTION FROM THE DEPARTMENT OF CHEMISTRY,
THE UNIVERSITY OF MICHIGAN, ANN ARBOR, MICHIGAN 48104

Vibrational Spectra and Assignments for Isotopic Species of Tetraborane(10)[1]

BY ALTON JOE DAHL AND ROBERT COOPER TAYLOR*[2]

Received February 16, 1971

Four isotopically enriched species of tetraborane(10) have been prepared involving hydrogen, deuterium, boron-10, and boron-11. The infrared spectra of these compounds have been investigated in the gas and solid states in the spectral region from 400 to 4000 cm^{-1}. Low-resolution Raman spectra in the liquid and solid states have been obtained and qualitative polarization measurements made. Vibrational modes of this molecule have been described on the basis of a symmetry analysis and a group vibration approximation. Tentative vibrational assignments have been made for 34 of the 36 fundamentals.

Introduction

Despite the extensive chemical interest in the boron hydrides and the intriguing nature of the hydrogen bridge bond which these compounds contain, spectroscopic attention has been focused almost entirely upon the simplest member of the series, diborane. Experimental difficulties caused by the reactive nature and general thermal instability of the higher hydrides, together with spectroscopic complications inherent in their relatively large size and the lack of isotopic purity of natural boron, seem to have been effective deterrents to study. These compounds clearly deserve considerably more attention than they have been accorded.

In the present work, the vibrational spectra of four isotopic varieties of tetraborane (10), B_4H_{10}, have been investigated in the gas, liquid, and solid states under low resolution in order to arrive at a preliminary set of vibrational assignments. The infrared spectrum of this compound prepared from boron containing the natural isotopic abundance has been reported in the literature, the most detailed results being those of Spielman and Burg,[3] who published the infrared spectrum of the vapor for both the hydrogen and deuterium compounds. Qualitative assignments were given based on frequency shifts and analogies with the spectra of other compounds. No Raman data have been found. A few infrared frequencies for the mixed isotopic species, $B_4H_8D_2$, have also been reported.[4] The only other higher boron hydride which has been given any signifi-

---

[1] Based on a dissertation submitted by A. J. Dahl in partial fulfillment of the requirements of the Ph.D. degree to the Horace H. Rackham School of Graduate Studies of The University of Michigan.

[2] Author to whom correspondence should be addressed.

(3) J. R. Spielman and A. B. Burg, *Inorg. Chem.*, **2**, 1139 (1963).

(4) A. D. Norman and R. Schaeffer, *J. Amer. Chem. Soc.*, **88**, 1143 (1966).

cant amount of spectroscopic study is pentaborane-(9).[5,6]

Experimental Section

The isotopic composition of natural boron, which has a 4:1 ratio of boron-11 to boron-10, introduces a number of complications into the vibrational spectra of boron hydrides prepared from natural material. Since most of the molecules in such a sample will have an actual symmetry less than the geometrical symmetry, selection rules will be relaxed and splitting of bands or isotopic satellites will occur. Under low resolution, the latter effects may result only in a general broadening of the bands, but asymmetric line shapes and unresolved shoulders may also be observed. Further effects may be greater difficulties in distinguishing overlapping fundamentals and significant shifts in the positions of apparent band maxima. Since the mass difference for the two boron isotopes is nearly 10%, the problems are not insignificant. To minimize such effects and aid the interpretation of the results, hydrogen and deterium species of tetraborane isotopically enriched in boron-10 and also boron-11 were synthesized for the present investigation. The extent of isotope mixing in molecular species based on the overall isotopic composition is indicated in Table I which compares natural boron with the enriched compositions used in the present work.

TABLE I

STATISTICAL DISTRIBUTION OF VARIOUS ISOTOPIC SPECIES IN TETRABORANE ASSUMING EQUAL *a priori* PROBABILITIES

	Boron-enriched compounds				
Isotope enrichment	$^{10}B_4$ (1)[a]	$^{10}B_3{}^{11}B$ (2)	$^{10}B_2{}^{11}B_2$ (3)	$^{10}B^{11}B_3$ (2)	$^{11}B_4$ (1)
92% ^{10}B	0.716	0.249	0.033	0.002	0.000
80% ^{11}B	0.002	0.026	0.154	0.409	0.409
99.4% ^{11}B	0.000	0.000	0.000	0.024	0.976
	Deuterium-enriched compounds				
	D_{10} (1)*		D_9H (4)		D_8H_2 (17)
97% D	0.737		0.228		0.032

[a] Numbers in parentheses indicate the number of nonidentical species which have the given mixture of isotopic atoms.

Preparation of Compounds.—Boron trifluoride enriched to 99.4 atom % ^{11}B or to 92 atom % ^{10}B was prepared by the thermal decomposition of the correspondingly enriched potassium fluoroborate and converted to the ethyl ether complex. The latter was then reduced by a mixture of LiH and $LiAlH_4$ in ether solution to give the enriched diborane. Ninety-seven per cent enriched LiD plus $AlCl_3$ was used for the deuterated material. The diborane was converted into an approximately equimolar mixture of tetraborane and pentaborane(11) by circulating it continuously through a thermal reactor held at 125° followed by a trap maintained at −78°. After 1 hr, during which time the pressure in the system slowly increased to nearly 2 atm from the production of hydrogen, the −78° trap was replaced with one at −196° and the hydrogen pumped off. The trap was then rewarmed to −78° and circulation continued. After four such cycles, a typical preparation produced 5 mmol of a mixture of tetraborane(10) and pentaborane(11) from an initial 17 mmol of diborane. The product mixture was separated by repeated trap-to-trap distillations and the purity of the tetraborane established by vapor pressure measurements and infrared spectra. Purified samples were stored at liquid nitrogen temperatures until used.

Spectroscopic Equipment and Procedures.—Infrared spectra were recorded with a Perkin-Elmer Model 21 spectrophotometer equipped with CaF_2, NaCl, and KBr prisms using indene lines for calibration. Gases were examined in a 10-cm cell with KBr windows. Solids were in the form of thin nonscattering films deposited from the vapor on a KBr plate maintained near liquid nitrogen temperatures in an evacuated cell.

Raman spectra of the samples were recorded photographically using a Gaertner two-prism instrument having a dispersion of about 180 cm^{-1}/mm in the blue region. Under the conditions of the experiments, the resolution attained was about 10 cm^{-1}. The most intense bands were also photographed under higher resolution using a Bausch and Lomb 1.5-m grating instrument. For the liquids, a Toronto type mercury arc source was used with which the temperature of the samples could be maintained at about −80°.[7] Sample volumes were in the range of 0.1–0.3 ml.

Details of the experimental apparatus and arrangement for the solid samples are available elsewhere.[8] Briefly, two Type AH-4 mercury arc lamps were used to supply Hg 4358 Å radiation. High spectral purity was obtained by passing the light through two narrow band pass multilayer filters after which it was focused on the sample contained in a 5-mm o.d. Pyrex tube. This tube was in good thermal contact with two heavy copper supports attached directly to a liquid nitrogen reservoir. Thermocouple measurements indicated that sample temperatures were below −160°.

To reduce the high intensity of incident radiation scattered from the polycrystalline samples, the scattered light was passed into the spectrograph *via* a discrimination unit which greatly reduced the relative intensity of the exciting radiation. This unit consisted of two parallel multilayer dielectric interference filters having a band pass maximum at 4358 Å. The scattered light from the sample was multireflected between the parallel faces before entering the spectrograph. At each reflection, approximately 70% of the 4358-Å radiation was removed by transmission through the filter surface, but, due to the interference nature of the filters, better than 98% of the Raman radiation was reflected. On the basis of six reflections, it was calculated that less than 0.1% of the 4358-Å light entering the discrimination unit reached the spectrograph slit whereas the Raman radiation was attenuated only to about 75% of the incident. The use of dielectric filters for this purpose has been described previously[9,10] but fewer reflections were employed. This technique not only made it possible to obtain good-quality spectra from polycrystalline samples but also markedly reduced the width of the Rayleigh line in the spectra of the small liquid samples (Figure 1).

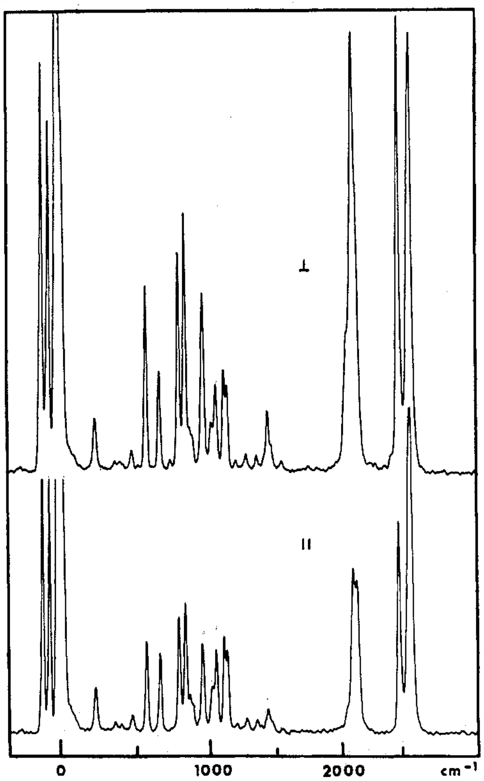

Figure 1.—Polarized Raman spectra of liquid $^{10}B_4H_{10}$ at −80°.

Frequencies of the Raman bands were determined from measurements on both the plates and microphotometer tracings using a fourth-degree polynomial fitted to standard argon lines. Esti-

---

(5) H. J. Hrostowski and G. C. Pimentel, *J. Amer. Chem. Soc.*, **76**, 998 (1954).

(6) S. R. Coriell and W. J. Taylor, Symposium on Molecular Structure and Spectroscopy, The Ohio State University, June 1964.

(7) G. L. Vidale and R. C. Taylor, *J. Amer. Chem. Soc.*, **78**, 294 (1956).

(8) A. J. Dahl, Dissertation, The University of Michigan, 1963.

(9) J. Brandmuller, *Z. Angew. Phys.*, **5**, 95 (1953).

(10) R. L. Amster and R. C. Taylor, *Spectrochim. Acta*, **20**, 1487 (1964).

TABLE II
OBSERVED INFRARED AND RAMAN FREQUENCIES OF $^{10}B_4H_{10}$ AND $^{11}B_4H_{10}$

$^{10}B_4H_{10}$				$^{11}B_4H_{10}$				
Infrared		Raman		Infrared		Raman		
Gas	Solid	Liquid	Solid	Gas	Solid	Liquid	Solid	Assignment
			2595 vvs					
2590 vvs	2588 vs	2583 vvs(p)	2585 vs,sh	2570 vvs	2575 vvs	2566 vvs(p)	2562 s	$\nu_1,\nu_2,\nu_{20},\nu_{28}$
	2570 vvs				2550 vvs			
2495 vvs	2486 vvs	2494 vvs(p)	2495 vvs	2485 vs	2475 vvs	2490 vvs(p)	2488 vs	ν_3,ν_{29}
	2436 w,sh		2439 vvw					
					2285 vvw			$2(\nu_7,\nu_{33})$
2285 w	2268 m			2270 w	2255 w			$\nu_{23} + \nu_{32}$
					2205 vvw			$\nu_{32} + \nu_{33}$
					2165 s			$\nu_{16} + \nu_{33}$
2150 vs	2138 vvs	2149 vvs	2150 s,sh	2150 vs	2130 vvs	2136 vs	2133 m	$\nu_{13},\nu_{21},\nu_{30}$
	2126 vvs							
	2091 s	2116 vvs(p)	2116 vvs		2095 vs	2107 vvs(p)	2106 s	ν_4
					2085 sh			$\nu_{16} + \nu_{32}$
	2070 sh	2071 w	2066 m		2060 sh	2069 m	2073 w	$\nu_{18} + \nu_{23}$
					2040 sh			$\nu_{23} + \nu_{25}$
					1985 vw			$\nu_{10} + \nu_{16}$
	1996 vw				1970 vw,br			$\nu_{11} + \nu_{33}$
	1956 vvw				1944 vw			
					1924 sh			$2\nu_{15}$
	1894 vvw				1870 vvw			$\nu_{16} + \nu_{25}$
1870 vvw	1868 w			1850 vvw	1854 w			$\nu_{17} + \nu_{34}$
1850 vvw	1845 vvw							
					1825 vvw			$\nu_{18} + \nu_{24}$
					1815 sh			$2\nu_8$
	1810 vvw							$2\nu_{34}$
					1783 vvw			$\nu_{11} + \nu_{17}$
					1750 vw	1747 vvw	1762 vw	$\nu_9 + \nu_{10}$
	1774 vw	1766 vvw			1730 vw			$\nu_8 + \nu_{11}$
1750 vvw,br	1753 w				1720 sh			$\nu_{11} + \nu_{34}$
	1735 vw,sh							$\nu_7 + \nu_{12}$
	1697 vw				1690 br			$2\nu_{25}$
					1670 vw			$\nu_{11} + \nu_{25}$
					1651 sh			$\nu_9 + \nu_{18}$
					1625 vvw			$\nu_{12} + \nu_{32}$
					1618 sh			$\nu_7 + \nu_{35}$
					1599 vw			$\nu_9 + \nu_{11}$
	1594 vw				1578 vvw			$\nu_{12} + \nu_{16}$
					1561 vvw			$2\nu_9$
	1540 w,br	1553 vw(p)			1531 sh	1529 vw(p)		$\nu_{32} + \nu_{35}$
					1515 w			$\nu_{12} + \nu_{15}$
		1485 vw			1475 w	1465 vvw		$\nu_8 + \nu_{12}$
	1461 m	1454 w(p)	1456 vw	1445 vw(A,C)	1444 m	1439 vw(p)		ν_5
	1435 vw	1430 vvw	1433 vvw		1422 w			$\nu_{12} + \nu_{18}$
	1424 vw				1403 m			$\nu_{12} + \nu_{25}$
1407 s	1410 vw			1395 s(A,C)	1388 vs			ν_{31}
	1380 vvw							$\nu_9 + \nu_{12}$
		1373 vw	1375 vvw		1351 vw	1353 vw		$\nu_{34} + \nu_{35}$
	1361 vvw				1343 vvw			$\nu_9 + \nu_{12}$
	1343 s				1324 m			ν_{14} or ν_{22}
	1318 m				1308 m			ν_{14} or ν_{22}
		1296 vw	1297 vvw					$\nu_{32} + \nu_{36}$
					1288 m			$\nu_5 + \nu_{35}$
1279 vvw	1269 vw			1258 w(A,C)	1255 s			ν_6
1219 vw	1218 m	1219 vvw	1228 vvw		1217 sh			$\nu_{10} + \nu_{36}$
1209 vw	1211 s			1196 m,sh	1196 s			ν_{29}
1173 w	1171 s			1153 s,sh	1154 m			$\nu_8 + \nu_{36}$
1156 w	1157 vs	1156 m	1155 w		1145 s	1149 m	1144 w	ν_7, ν_{33}
1142 vs(A,C)	1152 vs			1140 vs(A,C)				
	1128 sh				1134 m			$\nu_{34} + \nu_{36}$
	1124 vs	1127 m	1129 m	1116 w,sh	1117 s	1121 w	1118 w	ν_{15}
1071 m	1071 vs	1071 m	1075 m	1070 s(A,C)	1064 vs	1065 m	1062 w	ν_{32}
						1041 w	1041 vw	$\nu_{12} + \nu_{35}$?
	1042 vs	1038 m	1037 w		1023 s			ν_{16}
	989 vvw							$\nu_{18} + \nu_{36}$
974 vs	964 vvs	975 s(P)	975 s	966 vs	959 vvs	965 s(P)	964 w	ν_{10},ν_{24}
					929 vw	940 vvw		$2\nu_{35}$
916 vw	917 vs			910 vw	908 vs			ν_8
905 w	906 vs	901 vw	906 vw	895 w	898 vs	898 vw		ν_{34}
	872 vs	882 vw	885 vw		868 vs	867 vw		ν_{17}
854 vs(A,C)	854 vvs			848 s(A,C)	846 vvs			ν_{25}
		850 vs(p)	853 m		824 vvw	827 vs(p)	825 m	ν_{11}
	805 sh				798 m			$\nu_{12} + \nu_{36}$
800 w	802 s	805 s(p)	806 s	780 w,sh	783 m	785 s(p)	784 s	ν_9
	754 s	748 vvw	750 vvw		737 m			ν_{18}
					703 vvw			$\nu_{35} + \nu_{36}$
	682 vvw	672 m	680 m		662 w	659 m	650 w	ν_{19}
					617 vvw			?
	575 vs	579 s(p)	584 m	550 m	559 vs	558 s(p)	557 w	ν_{12}
						497 vvw		?
	474 s	483 vw		470 w	480 s	472 vw		ν_{35}
	415 vvw	409 vvw				413 vvw		?
		366 vvw				372 vvw		?
		238 m				236 m		ν_{36}

mated uncertainties are about 2 cm^{-1} for the more intense peaks and somewhat greater for the weaker ones. The uncertainties in the maxima of the infrared absorption bands are approximately the same.

Results

Observed vibrational frequencies for the four isotopic varieties of tetraborane in the gas, liquid, and solid states are listed in Tables II and III. Polarized Raman spectra of $^{10}B_4H_{10}$ and $^{10}B_4D_{10}$ are shown in Figures 1 and 2 in the form of microphotometer tracings. Figure 3 shows the vapor and solid spectra of the hydrogen and deuterium compounds prepared from boron-11.

X-Ray diffraction studies on the solid[11] have shown that the boron skeleton of tetraborane consists of two triangles of boron atoms which share a common edge

---

(11) C. E. Nordman and W. N. Lipscomb, *J. Chem. Phys.*, **21**, 1856 (1953). See also E. B. Moore, R. E. Dickerson, and W. N. Lipscomb, *ibid.*, **27**, 209 (1957).

TABLE III
OBSERVED INFRARED AND RAMAN FREQUENCIES OF $^{10}B_4D_{10}$ AND $^{11}B_4D_{10}$

$^{10}B_4D_{10}$				$^{11}B_4D_{10}$				
Infrared		Raman		Infrared		Raman		
Gas	Solid	Liquid	Solid	Gas	Solid	Liquid	Solid	Assignment
2597 sh	2585 m		2596 vw		2583 vvw		2587 vvw	H impurity
2568 m					2546 sh		2544 vvw	" "
	2540 sh	2555	2545 vvw	2525 vw	2535 vw			" "
2528 w	2530 m				2511 vvw			" "
	2500 m	2516	2509 vvw		2498 vvw		2498 vvw	" "
	2285 vvw							" "
2137 vw	2135 m	2143	2142 vvw	2120 vvw	2130 vvw,br		2129 vvw	" "
	2055 vvw							
1946 vvs	1956 vvs	1953 vvs(p)	1950 vvs	1946 vvs	1932 vvs	1934 vvs	1933 vvs	$\nu_{1},\nu_{2},\nu_{20},\nu_{28}$
	1940 sh							$\nu_{10}+\nu_{31}$
	1900 s	1908			1894 vw,sh			$2\nu_{6}$
					1885 vw			$\nu_{31}+\nu_{33}$
	1876 s	1872	1883 vw		1855 vvw		1859 vw	$\nu_{10}+\nu_{14}$
	1869 sh							$\nu_{6}+\nu_{23}$
1826 vs	1834 vs	1834 vvs(p)	1832 vs	1826 vs	1821 vvs	1825 vvs	1821 vvs	ν_{3}, ν_{29}
					1778 vvw			$\nu_{11}+\nu_{22}$
1775 vvw	1767 m		1771 vvw	1720 vvw,br	1736 vvw			$\nu_{6}+\nu_{11}$
	1707 sh							$\nu_{5}+\nu_{25}$?
	1702 sh							$\nu_{10}+\nu_{32}$?
	1697 m							$2\nu_{7}, \nu_{17}+\nu_{22}$?
	1683 sh							$\nu_{10}+\nu_{16}$
	1667 vvw							$\nu_{9}+\nu_{14}$
1583 vs	1582 s	1598 vvs	1594 sh	1583 vs	1572 vvs	1585 vvs	1582	$\nu_{13},\nu_{21},\nu_{30}$
	1570 sh	1568 vvs(p)	1567 vvs		1559 sh		1557 vw	ν_{4}
					1535 vw			$\nu_{7}+\nu_{17}$
	1544 w					1517 w		$2\nu_{16}$
	1536 sh							$\nu_{8}+\nu_{24}$
	1529 sh							$\nu_{8}+\nu_{32}$
	1508 vvw							$\nu_{9}+\nu_{11}$
	1496 vvw							$\nu_{10}+\nu_{19}$
	1478 sh				1457 vvw			$2\nu_{8}$
	1461 vvw							$\nu_{9}+\nu_{16}$
	1442 vvw				1425 vvw			$2\nu_{34}$
	1419 sh							H impurity
	1410 vvw							$\nu_{9}+\nu_{34}$
	1390 vw			1375 vvw,br	1382 vvw			$\nu_{23}+\nu_{27}$?
1370 vvw,br	1370 w				1360 vw			$\nu_{25}+\nu_{34}$
	1350 w				1333 vvw			$2\nu_{18}$
	325 vw							$\nu_{12}+\nu_{32}$
					1311 vvw			$\nu_{12}+\nu_{24}$
	1310 vvw							$2\nu_{25}$
	1299 vvw				1281 vvw			$\nu_{12}+\nu_{16}$
	1286 vvw							$\nu_{17}+\nu_{19}$
	1263 sh							$\nu_{8}+\nu_{12}$
	1258 vvw							$\nu_{16}+\nu_{26}$?
	1218 vvw,br				1181 vvw			$\nu_{9}+\nu_{12}$
	1192 vvw							$\nu_{22}+\nu_{36}$
	1175 vw				1166			$\nu_{12}+\nu_{25}$
	1157 w				1151 vvw			$\nu_{8}+\nu_{35}$
					1138 vvw			$\nu_{6}+\nu_{36}$
	1097 w							$\nu_{18}+\nu_{35}$
	1055 m				1046 m			ν_{5}
1035 m	1032 s,br	1035 vvw		1030 m	1029 w			ν_{31}
	997 s				986			ν_{14} or ν_{22}
	977 s	979 vvw			969 w			ν_{14} or ν_{22}
	963 w				958			$\nu_{16}+\nu_{36}$?
	952 m			948 vvw	946 vw,br			ν_{6}
	942 w				928 vvw			$\nu_{12}+\nu_{35}$?
	923 w		924 vvw		901 vw			ν_{23}
	901 vw				894 sh			$\nu_{34}+\nu_{36}$
	911 vw	910 m				888 m(p)	901	ν_{10}
	893 vw			885 vvw	884 sh			$\nu_{17}+\nu_{36}$
					872 sh			?
855 s(A,C)	850 vvs	849 vw	856 m	850 s(A,C)	842 vs	842 vw	843 vvw	ν_{7}, ν_{33}
	827 sh		828 sh		806 sh			?
	801 sh				801 sh			?
	820 w	816 s				795 s (p)	801 m	ν_{11}
805 s	806 vs			795 m	794 s			ν_{24}
	794 s				781 m			ν_{32}
	773 m				763 m			ν_{16}
	753 vvw							?
737 w	736 m		737 vvw		730 m		739 w	ν_{8}
					726 sh			?
725 m	718 m	724 m	728 m	720 w	714 m	715 m	717 vs	ν_{34}
	704				697 w			ν_{17}
					683 vvw			$\nu_{27}+\nu_{36}$?
	693 vw	692 m				667 m	669 m	ν_{9}
	678 vvs		680 vw		670 s			ν_{18}
650 s	656 vvs	656 m	670 w	648 M(A,C)	651 s	648 m	656 m	ν_{25}
					643 sh			?
					628 sh			?
	630 vw				622 w			$\nu_{35}+\nu_{36}$?
	602 vvw							?
	589 vvw	582 w	585 w			570 w	580 m	ν_{19}
	532 w	534 s	540 m		519 w	516 s	528 s	ν_{12}
	515 w				505 vw			ν_{26}?
	503 sh				497 vvw			?
	494 vs	489	495		487 vs			ν_{27}?
	463 vw							?
	438 sh							?
	433 m	430 vvw			426 m	420 vvw		ν_{35}?
		195 w						ν_{36}?

and two atoms as shown in Figure 4. Two terminal hydrogens are attached to each of the end (unshared) boron atoms and a single terminal hydrogen is attached to each of the central borons. Four bridging hydrogen atoms are located around the periphery of the boron skeleton.

On the basis of the X-ray results, the free molecule is presumed to have C_{2v} symmetry and is expected to be an

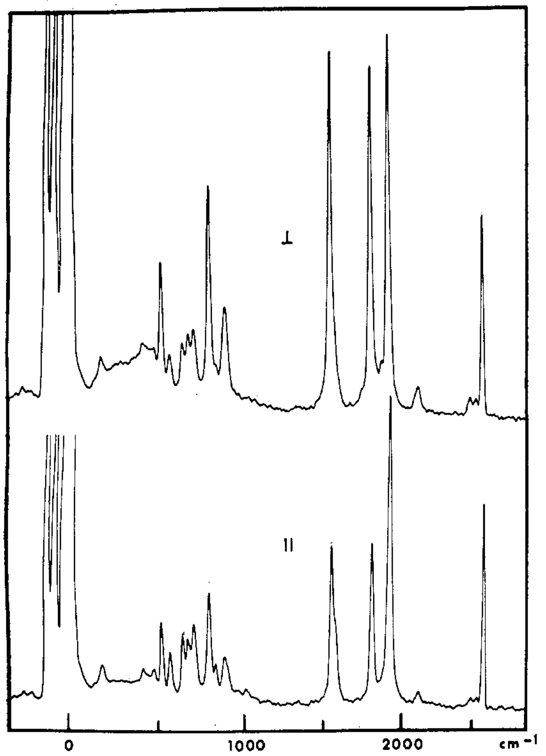

Figure 2.—Polarized Raman spectra of liquid $^{10}B_4D_{10}$ at −80°.

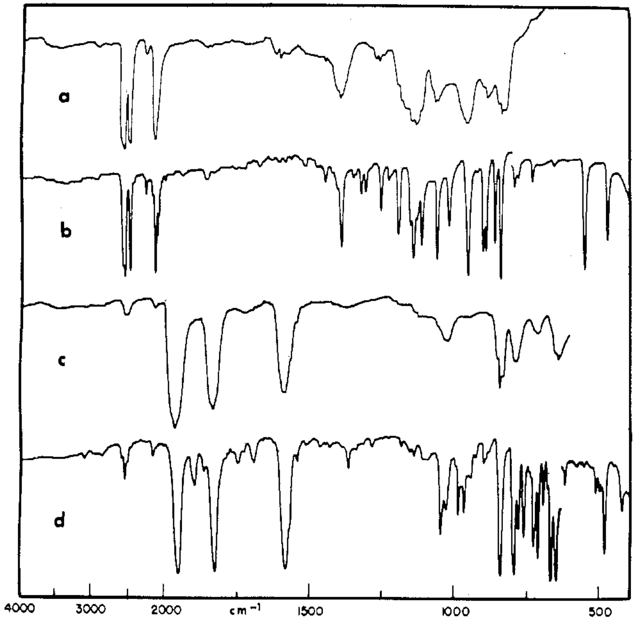

Figure 3.—Infrared spectra of tetraborane: (a) $^{11}B_4H_{10}$ vapor; (b) $^{11}B_4H_{10}$ solid at −180°; (c) $^{11}B_4D_{10}$ vapor; (d) $^{11}B_4D_{10}$ solid at −180°.

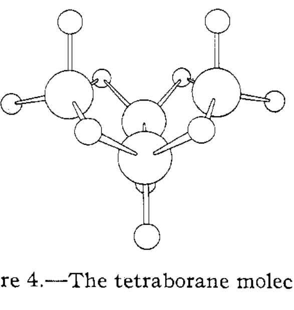

Figure 4.—The tetraborane molecule.

asymmetric rotor. Calculations using the X-ray parameters show that the axis of the least moment of inertia extends lengthwise of the molecule in the plane of the two BH_2 groups and perpendicular to the C_2 axis. The largest moment of inertia is around the C_2 axis with the intermediate moment axis perpendicular to the C_2 axis and in the plane containing the two single terminal hydrogens. It is customary to classify the infrared band shapes of C_{2v} molecules into A, B, or C type bands depending on whether the vibrational motion involved produces a dipole moment change along the least, intermediate, or largest axis of inertia, respectively. These three types of vibration–rotation bands have fairly characteristic shapes which depend to some extent on the ratios of the various moments. Type A bands, for example, exhibit a strong central Q branch with fairly pronounced P and R branches on either side, a shape which is largely independent of the ratios of moments. Vibrations giving rise to A type bands will belong to the B_2 symmetry class of the B_4H_{10} molecule with the dipole moment change occurring along the least axis of inertia. Type B bands characteristically show a doublet structure due to the P and R branches since no Q branch is present. The P and R branches may be somewhat broad and diffuse. Type B bands in the present molecule are identified with the B_1 symmetry class. The shape of type C bands is strongly dependent on the ratio of the two smaller moments of inertia. If this ratio is greater than about 0.2, however, as is the case here, type C bands should have bands shapes similar to those of type A bands. Type C bands correspond to totally symmetric or A_1 vibrations since the dipole moment change is along the C_2 axis.

Experimental difficulties such as overlapping of bands, lack of resolution, perturbations, etc., may obscure band contours. However, a number of band shapes were sufficiently well defined in the present work to allow satisfactory identification. The spectra of the solids were noticeably more complex than those of the liquid or the gas. To a large degree, this was due to the increased sharpness of the bands at the lower temperatures which allowed composite bands to be resolved into their components. Further complexity was contributed by the relaxation of molecular selection rules, not to mention the possibility of additional lines from intermolecular interactions within the factor-group approximation. The space group of tetraborane is $C_{2h}{}^5$ with four molecules per unit cell. No attempt was made in the present work to extend the analysis to include crystal effects.

Vibrational Assignments

Assuming C_{2v} molecular symmetry, the vibrational modes of the B_4H_{10} molecule may be classified into twelve A_1, seven A_2, eight B_1, and nine B_2 frequencies. For the free molecule, the A_1, B_1, and B_2 classes are infrared active while all classes are Raman active. In the solid, the A_2 class becomes infrared active as well.

The various molecular vibrational modes can be described most easily in terms of idealized group motions involving the BH_2 groups, the BH groups, the hydrogen bridge atoms, and the boron atom skeleton. The numbering scheme and a description of the fundamentals in terms of these group motions appear in Table IV and a pictorial representation is shown in Figure 5 for addi-

TABLE IV

DESCRIPTIONS OF VIBRATIONAL MODES OF TETRABORANE

	Class A_1
ν_1	In-phase B–H str
ν_2	Sym out-of-phase BH_2 str
ν_3	Sym in-phase BH_2 str
ν_4	+ + + + in-phase bridge str
ν_5	+ + + + out-of-phase bridge str
ν_6	Out-of-phase BH def
ν_7	In-phase BH_2 sciss
ν_8	In-phase BH_2 rock
ν_9	+ + + + bridge def
ν_{10}	In-phase boron ring expansion
ν_{11}	Out-of-phase boron ring expansion
ν_{12}	Boron ring dihedral bend
	Class A_2
ν_{13}	+ − + − in-phase bridge str
ν_{14}	+ − + − out-of-phase bridge str
ν_{15}	Out-of-phase BH wag
ν_{16}	Out-of-phase BH_2 wag
ν_{17}	Out-of-phase BH_2 twist
ν_{18}	+ − + − bridge def
ν_{19}	Twist of B–B bond around C_2 axis
	Class B_1
ν_{20}	Out-of-phase BH str
ν_{21}	+ − − + in-phase bridge str
ν_{22}	+ − − + out-of-phase bridge str
ν_{23}	In-phase BH def
ν_{24}	In-phase BH_2 wag
ν_{25}	In-phase BH_2 twist
ν_{26}	+ − − + bridge def
ν_{27}	In-phase motion of BH groups parallel to B–B bond
	Class B_2
ν_{28}	Asym out-of-phase BH_2 str
ν_{29}	Asym in-phase BH_2 str
ν_{30}	+ + − − in-phase bridge str
ν_{31}	+ + − − out-of-phase bridge str
ν_{32}	In-phase BH wag
ν_{33}	Out-of-phase BH_2 sciss
ν_{34}	Out-of-phase BH_2 rock
ν_{35}	+ + − − bridge def
ν_{36}	In-phase motion of BH groups perpendicular to the B–B bond

TABLE V

FREQUENCY ASSIGNMENTS FOR THE FUNDAMENTAL VIBRATIONS OF TETRABORANE (CM^{-1})

	$^{10}B_4H_{10}$	$^{11}B_4H_{10}$	$^{10}B_4D_{10}$	$^{11}B_4D_{10}$	
		Symmetry Class A_1			
ν_1	2590	2570	1946	1946	BH str
ν_2	2590	2570	1946	1946	BH_2 str
ν_3	2486	2475	1834	1821	BH_2 str
ν_4	2116	2095	1570	1559	Bridge str
ν_5	1461	1444	1055	1046	Bridge str
ν_6	1269	1255	952	946	BH def
ν_7	1157	1145	850	842	BH_2 sciss
ν_8	917	908	736	730	BH_2 rock
ν_9	805	785	692	667	Bridge def
ν_{10}	975	965	910	888	Boron ring expansion
ν_{11}	850	827	816	795	Boron ring expansion
ν_{12}	575	559	532	519	Boron ring bend
		Symmetry Class A_2			
ν_{13}	2150	2150	1583	1583	Bridge str
ν_{14}	1318	1308	977	969	Bridge str
ν_{15}	1124	1117	...	...	BH wag
ν_{16}	1042	1023	773	763	BH_2 wag
ν_{17}	872	868	704	697	BH_2 twist
ν_{18}	754	737	678	670	Bridge def
ν_{19}	682	662	589	575	Skel twist
		Symmetry Class B_1			
ν_{20}	2590	2570	1946	1946	BH str
ν_{21}	2150	2150	1583	1583	Bridge str
ν_{22}	1343	1324	997	986	Bridge str
ν_{23}	1211	1196	923	901	BH def
ν_{24}	974	966	806	794	BH_2 wag
ν_{25}	854	846	656	651	BH_2 twist
ν_{26}	...	...	515	505	Bridge def
ν_{27}	...	...	494	487	Skel def
		Symmetry Class B_2			
ν_{28}	2590	2570	1946	1946	BH_2 str
ν_{29}	2486	2475	1834	1821	BH_2 str
ν_{30}	2150	2150	1583	1583	Bridge str
ν_{31}	1410	1388	1032	1029	Bridge str
ν_{32}	1071	1064	794	781	BH wag
ν_{33}	1152	1140	850	842	BH_2 sciss
ν_{34}	906	898	718	714	BH_2 rock
ν_{35}	483	472	430	420	Bridge def
ν_{36}	238	236	195	189	Skel def

tional clarity. These sketches may be considered a zero-order approximation to the normal coordinates and form a conveneint basis for discussion. A more accurate description must await a normal-coordinate analysis.

A summary of the frequency assignments for the fundamental vibrations of the four isotopic species of tetraborane is given in Table V. Symmetry assignments were based on a consideration of band shapes, polarization properties of the Raman bands, comparisons between infrared and Raman spectra, and comparisons between gas and crystal spectra. Assignments within a symmetry class were made on the basis of boron and deuterium isotope shifts and by comparisons with published assignments of diborane[12–15] and pentaborane(9).[5] For uniformity, the frequency values cited in the Discussion sections to follow refer to the $^{10}B_4H_{10}$ species unless specific mention is made of another.

B–H and BH_2 Stretching Vibrations.—The out-of-phase stretching frequency of the BH_2 group and also the stretching frequency of a single terminal hydrogen on boron, from the work on diborane and pentaborane(9), have both been located at about 2600 cm^{-1}. In tetraborane, since neither the two BH groups nor the two BH_2 groups are closely coupled with each other, little separation may be expected between these stretching modes. The band at about 2590 cm^{-1} obviously is complex and consequently all four fundamentals, ν_1, ν_2, ν_{20}, and ν_{28}, are assigned to this peak. In diborane, the two in-phase BH_2 vibrations have been assigned to frequencies at about 2525 cm^{-1}. By analogy, the 2495-cm^{-1} band in the infrared spectrum of gaseous tetraborane is delegated to ν_3 and ν_{29}.

Bridge Stretching Vibrations.—The bridge modes expected to have the highest frequency are those in which the two bonds connected to each bridge atom stretch in phase. By analogy with diborane, the in-phase stretching frequencies were sought around 2100 cm^{-1}. The band at 2116 cm^{-1} in the tetraborane Raman spectrum was observed to be strongly polarized and is therefore assigned to ν_4; the other three modes, ν_{13}, ν_{21}, and ν_{30}, are thought to be contained in the infrared band with its maximum at 2150 cm^{-1} in the spectrum of the gas.

The remaining bridge modes are those in which the two bonds connecting given bridge hydrogen atoms stretch out of phase. These were more difficult to assign since this type of vibration, based on the few data that are

---

(12) R. C. Lord and E. Nielsen, *J. Chem. Phys.*, **19**, 1 (1951).

(13) R. C. Taylor and A. R. Emery, *Spectrochim. Acta*, **10**, 419 (1958).

(14) I. M. Mills, *J. Chem. Phys.*, **41**, 1479 (1964).

(15) W. J. Lafferty, A. G. Maki, and T. D. Coyle, *J. Mol. Spectrosc.*, **33**, 189 (1970).

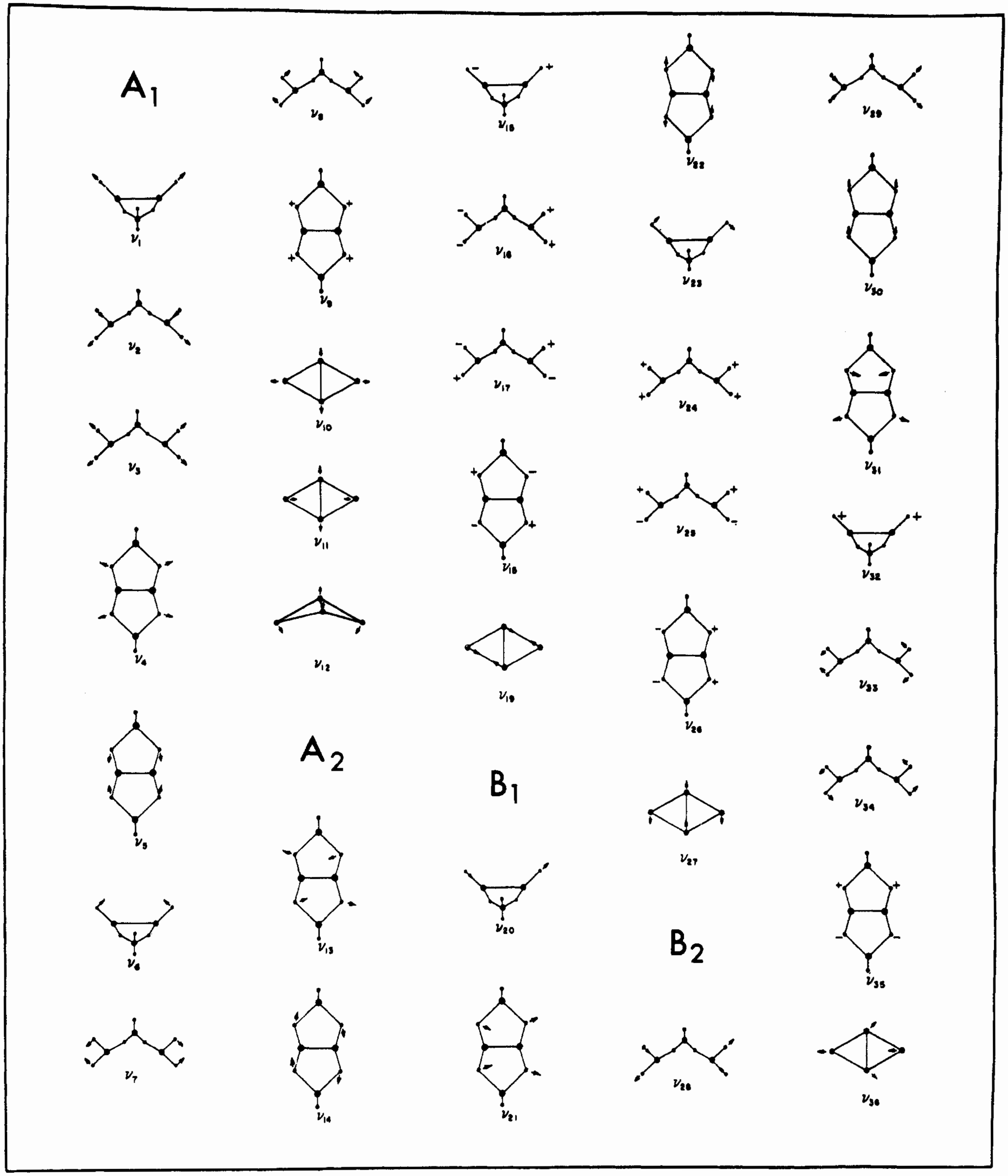

Figure 5.—Approximate normal modes for the tetraborane molecule based on equivalent atom sets.

available, appears to vary significantly from compound to compound and is more easily influenced by the rest of the molecule. The easiest band to assign of this group was ν_5 which was assigned to a polarized Raman frequency at 1454 cm^{-1}. In the infrared spectrum several lines occur in this region. The most intense of these at 1407 cm^{-1} has a band shape suggestive of either a type A or C band and consequently is assigned to the B_2 fundamental. The remaining two modes are assigned with less certainty. However, the two bands at 1318 and 1343 cm^{-1} were observed in the infrared spectrum of the solid and not of the gas and are tentatively assigned as the A_2 and B_1 out-of-phase stretches, ν_{14} and ν_{22}, respectively. A fairly large change in relative intensity of these two bands occurs upon substitution of boron-11 for boron-10 which may indicate resonance with overtones or combinations of lower frequencies.

BH_2 Bending Vibrations.—In diborane, the two BH_2

scissoring modes have been assigned at 1177 and 1180 cm^{-1}. In tetraborane, an intense band having several maxima occurs at 1155 cm^{-1} in the infrared spectrum of the solid. This band correlates with a relatively simple band at 850 cm^{-1} in the spectrum of B_4D_{10} vapor. The latter appears to possess an A or C type of band envelope indicating a B_2 or A_1 vibration. The band is assigned to both ν_7 and ν_{33}. The complexity of the band in the spectrum of the hydrogen species is attributed to interactions with overtones and combinations.

The two BH_2 wagging motions of diborane have frequencies of 973 and 1035 cm^{-1}. In solid tetraborane, the infrared spectrum exhibits a number of strong bands from 1124 to 854 cm^{-1}. Of these, the three at 1124, 1042, and 872 cm^{-1} appear to be absent in the spectrum of the gas and are candidates for A_2 frequencies while the frequency at 974 cm^{-1} does not show a central Q branch in the gaseous spectrum indicative of symmetry class B_1. Since one would not expect the BH_2 wagging frequencies of tetraborane to be markedly different from those of diborane, the frequencies at 1042 and 974 cm^{-1} are assigned, respectively, to ν_{16} and ν_{24}.

The two BH_2 rocking modes of tetraborane, ν_8 and ν_{34}, belonging to symmetry classes A_1 and B_2 are assigned to infrared bands at 917 and 906 cm^{-1}, respectively, by analogy with the corresponding modes in diborane at 950 and 920 cm^{-1}.

The lowest bending modes of the BH_2 groups are the twisting motions, ν_{17} and ν_{25}, which are assigned to infrared bands at 872 and 854 cm^{-1}. The first is characterized as A_2 by its absence in the gas infrared spectrum and its presence in that of the solid. The second can be classified as A_1 or B_2 by its band shape which is either type A or C. In diborane, corresponding modes occur at 1012 and 829 cm^{-1}.

BH Bending Vibrations.—Although the infrared and Raman spectra of decaborane(14)[16] indicate that no BH deformation modes occur in that molecule higher than 1104 cm^{-1}, greater coupling may be expected in B_4H_{10} and the frequencies may not be as low. Of the four fundamentals involving the deformation of the single terminal hydrogens, ν_6 and ν_{23} belong to the classes A_1 and B_1. The A_1 vibration is assigned to the infrared band at 1269 cm^{-1} which shows definite PQR branches in the spectrum of the gas. The B_1 mode is delegated to the infrared frequency at 1211 cm^{-1}, primarily because it is the only intense peak in this region which remains unassigned. The other two modes, ν_{15} and ν_{32}, belong to the A_2 and B_2 classes and are assigned to bands at 1124 and 1071 cm^{-1}, respectively. The first is chosen as the A_2 band because of its absence in the gaseous infrared spectrum and its presence in that of the solid. The other band shows a band shape consistent with that expected for the B_2 symmetry class.

Skeletal Vibrations and Bridge Deformation Modes.—Four types of internal coordinates are appropriate to describe these modes—the B–B distances, the bridge BHB angles, and the dihedral angles between the planes defined by the BHB atoms and the attached BBB triangle, and between the two BBB triangles. Changes in the first, third, and fourth types of coordinates combine to give the skeletal modes labeled ν_{10}, ν_{11}, ν_{12}, and ν_{19} in Table IV. The remaining coordinates are those involved primarily in the vibrations designated as bridge deformations. Since all these coordinates are defined essentially by the same atoms it is highly likely that the normal modes involving them are strongly mixed. Support for this conclusion is found in the observation that most of the bands below 800 cm^{-1} have hydrogen: deuterium ratios intermediate between those expected for "pure" hydrogen motions and "pure" skeletal motions.

The four frequencies of these two types belonging to the A_1 class were identified by their polarization properties in the Raman spectrum. The frequencies ν_9, ν_{10}, ν_{11}, and ν_{12} were assigned, respectively, to the Raman bands at 805, 975, 850, and 579 cm^{-1}. The order of the frequencies ν_{10}, ν_{11}, and ν_{12} was determined by a simplified numerical calculation assuming a simple model with only four boron atoms having the same configuration as diborane. Several different sets of force constants were tried but all gave the result that the in-phase ring stretching mode had a higher frequency than the out-of-phase mode. The polarized Raman line at 805 cm^{-1} assigned to ν_9 shows too small a shift upon deuteration to be a reasonably pure hydrogen motion. In addition, an unusually large change in intensity occurs between the spectra of the two isotopic species which seems to indicate significant coupling with ν_{11} in the hydrogen compound.

A fairly intense Raman line at 672 cm^{-1} is weak in the infrared spectrum of the solid and absent in the spectrum of the gas indicating that it probably is of A_2 symmetry. Since the H:D isotope frequency ratio is low (1.15), this band is assigned to the other skeletal mode, ν_{19}.

The remaining five frequencies associated with the skeleton and bridge hydrogen deformation motions have been designated only tentatively. No reliable information was obtained in the present work to distinguish them although bands considered likely to correspond to these various modes have been labeled in Tables II, III, and V.

Despite the fact that certain of the preceding assignments must be considered tentative, the amount of information provided to establish the symmetry species of many of the bands can serve as a solid basis for future work. The infrared results are incomplete below 400 cm^{-1} and further work involving oriented single crystals or matrix studies using higher resolution infrared and Raman spectroscopy is much to be desired.

The group frequency approach used here is likely to be most accurate for the normal modes primarily associated with the stretching and deformations of B–H bonds, somewhat less accurate for motions involving the bridge hydrogens, and poorest for the low-frequency motions which are probably complex in character. A normal-coordinate analysis would be necessary to gain further insight but unfortunately would not be a trivial task.

Acknowledgment.—The work reported here was supported in part by the National Science Foundation under Grants G-10372 and G-21408. The authors are indebted to Dr. P. H. Clippard for help in preparing the manuscript.

---

[16] R. C. Taylor, unpublished observations.